prevents this, harnessing the energy of GTP hydrolysis for protein targeting.

High-affinity interaction of SRP with ribosomes can occur before SRP interaction with the signal peptide when a short nascent chain is still inside the ribosome, raising the question of how SRP selectively targets signal sequence–containing substrates (*17*). Our results show that the interaction of the signal peptide with SRP accelerates SRP-SR complex formation, thereby providing a mechanism for selective delivery of appropriate substrates to the membrane. This is conceptually analogous to the kinetic mechanism by which translation achieves fidelity, where cognate codon-anticodon pairing accelerates GTP hydrolysis by elongation factor Tu (EF-Tu) (*18, 19*).

Our results provide an intuitive model for how each step of the targeting process activates the next to achieve productive, directional targeting. Signal peptides bind to SRP's conformationally flexible M domain that forms a continuous surface with SRP RNA (*8, 13*). Binding induces a conformational change that activates SRP RNA (*20*). Activated SRP RNA facilitates the displacement of the N-terminal helices of SRP and SR that slow their association without SRP RNA

(*21*). This commits the ribosome–nascent chain complex to membrane targeting. The kinetic control described here, where substrate recruitment accelerates downstream interactions, provides a generalizable principle for coordination of multistep pathways.

References and Notes
1. R. J. Keenan, D. M. Freymann, R. M. Stroud, P. Walter, *Annu. Rev. Biochem.* **70**, 755 (2001).
2. D. Zopf, H. D. Bernstein, A. E. Johnson, P. Walter, *EMBO J.* **9**, 4511 (1990).
3. J. D. Miller, H. Wilhelm, L. Gierasch, R. Gilmore, P. Walter, *Nature* **366**, 351 (1993).
4. P. Peluso, S. O. Shan, S. Nock, D. Herschlag, P. Walter, *Biochemistry* **40**, 15224 (2001).
5. T. Powers, P. Walter, *Science* **269**, 1422 (1995).
6. M. A. Poritz *et al.*, *Science* **250**, 1111 (1990).
7. P. Peluso *et al.*, *Science* **288**, 1640 (2000).
8. R. T. Batey, R. P. Rambo, L. Lucast, B. Rha, J. A. Doudna, *Science* **287**, 1232 (2000).
9. J. R. Jagath, M. V. Rodnina, W. Wintermeyer, *J. Mol. Biol.* **295**, 745 (2000).
10. X. Zhang, S. Kung, S. O. Shan, *J. Mol. Biol.* **381**, 581 (2008).
11. P. Walter, G. Blobel, *Proc. Natl. Acad. Sci. U.S.A.* **77**, 7112 (1980).
12. G. von Heijne, *J. Mol. Biol.* **184**, 99 (1985).
13. R. J. Keenan, D. M. Freymann, P. Walter, R. M. Stroud, *Cell* **94**, 181 (1998).
14. J. F. Swain, L. M. Gierasch, *J. Biol. Chem.* **276**, 12222 (2001).
15. J. H. Peterson, C. A. Woolhead, H. D. Bernstein, *J. Biol. Chem.* **278**, 46155 (2003).
16. See supporting material on *Science* Online.
17. T. Bornemann, J. Jockel, M. V. Rodnina, W. Wintermeyer, *Nat. Struct. Mol. Biol.* **15**, 494 (2008).
18. T. Pape, W. Wintermeyer, M. Rodnina, *EMBO J.* **18**, 3800 (1999).
19. J. M. Ogle, V. Ramakrishnan, *Annu. Rev. Biochem.* **74**, 129 (2005).
20. N. Bradshaw, P. Walter, *Mol. Biol. Cell* **18**, 2728 (2007).
21. S. B. Neher, N. Bradshaw, S. N. Floor, J. D. Gross, P. Walter, *Nat. Struct. Mol. Biol.* **15**, 916 (2008).
22. We thank J. Weissman, C. Gross, P. Egea, C. Gallagher, A. Korennykh, A. Acevedo, W. Weare, and J. Kardon for assistance and comments. Supported by NIH grant ROI GM32384 (P.W.), an NSF predoctoral fellowship (N.B.), the Jane Coffin Childs Memorial Fund (S.B.N.), and National Institute of General Medical Sciences fellowship R25 GM56847 (D.S.B.). P.W. is an Investigator of the Howard Hughes Medical Institute.

Floral Iridescence, Produced by Diffractive Optics, Acts As a Cue for Animal Pollinators

Heather M. Whitney,[1]* Mathias Kolle,[2,3]* Piers Andrew,[3] Lars Chittka,[4] Ullrich Steiner,[2,3]† Beverley J. Glover[1]†

Iridescence, the change in hue of a surface with varying observation angles, is used by insects, birds, fish, and reptiles for species recognition and mate selection. We identified iridescence in flowers of *Hibiscus trionum* and *Tulipa* species and demonstrated that iridescence is generated through diffraction gratings that might be widespread among flowering plants. Although iridescence might be expected to increase attractiveness, it might also compromise target identification because the object's appearance will vary depending on the viewer's perspective. We found that bumblebees (*Bombus terrestris*) learn to disentangle flower iridescence from color and correctly identify iridescent flowers despite their continuously changing appearance. This ability is retained in the absence of cues from polarized light or ultraviolet reflectance associated with diffraction gratings.

Biological iridescence results from various mechanisms, including multilayered materials, crystalline inclusions, and surface diffraction gratings (*1–6*). Diffraction gratings, surface striations of particular amplitude and frequency, cause interference, giving rise to an angular color variation (*7*). Although epidermal plant cell shape has been shown to influence the capture of all wavelengths of light by pigments (*8–10*), the mechanisms of iridescence have been poorly studied in plants; however, multilayered effects are occasionally observed in leaves (*11, 12*).

Hibiscus trionum petals are white with a patch of red pigment at the base. This pigmented patch is iridescent, appearing blue, green, and yellow depending on the angle from which it is viewed (Fig. 1, A and B). Scanning electron microscopy (SEM) shows a sharply defined difference between the surface structure overlying the pigment and the rest of the petal (Fig. 1C). This iridescence is visible to the human eye; however, in flowers with similar surface structures, such as many species of *Tulipa* (table S1), the iridescence is only evident to humans when the pigment color and petal surface structure are separated.

When the surface structure of hibiscus and tulip petals was replicated in colorless optical epoxy (*13*), iridescent color was visible independent of pigment (fig. S3A). SEM of these replicas showed that long, ordered, cuticular striations overlay the iridescent epidermal cells. These cuticular striations resemble a diffraction grating. The diffraction grating of compact discs (CDs) has been previously characterized (*7*), so we used SEM to compare an epoxy cast made from the plastic interior of a disassembled CD with a cast of *Tulipa kolpakowskiana* (Fig. 2, A and B). The tulip cast (Fig. 2, C and D) shows a rounded cross-section of the striations (as opposed to the square profile of the CD) and a long wavelength undulation with a periodicity of 29 ± 2 μm, reflecting the surface of the epidermal cells.

We further investigated the tulip casts with optical spectroscopy in the 300-to-900-nm wavelength range [near-ultraviolet (near-UV) to infrared]. A collimated light beam of ~2 mm in diameter was reflected off the cast at an incidence angle $\theta_I = 30°$, and the reflected and scattered light was detected at angles θ_D varying from 0° to 90° in 1° steps (fig. S1). The angular detection aperture was less than 1° [supporting online material (SOM) text].

The spectrally resolved reflectivity was determined for the tulip cast (Fig. 3, A and B),

[1]Department of Plant Sciences, University of Cambridge, Downing Street, Cambridge CB2 3EA, UK. [2]Department of Physics, Cavendish Laboratory, University of Cambridge, J. J. Thomson Avenue, Cambridge CB3 0HE, UK. [3]Nanoscience Centre, University of Cambridge, 11 J. J. Thomson Avenue, Cambridge, CB3 0FF, UK. [4]School of Biological and Chemical Sciences, Queen Mary University of London, London E1 4NS, UK.

*These authors contributed equally to this work.
†To whom correspondence should be addressed. E-mail: u.steiner@phy.cam.ac.uk (U.S.); bjg26@cam.ac.uk (B.J.G.)

a CD cast (Fig. 3C), and a planar reference sample (Fig. 3D). The reference shows only the specular signal at $\theta_D = 30°$ (sin $\theta_D = 0.5$) for all wavelengths. The CD cast additionally shows first-order interference (Fig. 3C, diagonal lines) and a weak second-order signal (Fig. 3C, bottom left), both of which are quantitatively described by the grating equation $m\lambda = d(\sin \theta_D - \sin \theta_I)$, where λ is the wavelength of light, d is the pe-riodicity of the grating ($d = 1.45$ μm), and m is the diffraction order (*14*).

The optical signature of the tulip cast (Fig. 3A) was more complex. The first-order diffraction signal was clearly visible at large angles (sin $\theta_D > 0.7$). It is broadened as compared with that of the CD because of the surface undulation (that is, the cells) shown in Fig. 2D. The two lines in Fig. 3A, which we calculated with the grating equation, delimit the predicted spectral range of first-order diffraction for such a wavy surface (SOM text). Compared with Fig. 3, C and D, the specular reflection is broadened and shows an intensity decrease toward long wavelengths. This is a combination of the ~30-μm surface undulation and the overall disorder in the pattern of the epidermal cells. Most of the optical intensity is at short wavelengths, coinciding with the high sensitivity of the bee eye in the blue and near-UV (*15*) ranges. UV signals caused by iridescence are known in animals (*3, 16, 17*). Furthermore, bees recognize contrasting patterns in the UV range that occur on flowers (*18*). Therefore, the optical signature and its angular dependence, because of its particular strength in the UV range, may be even more meaningful in terms of insect vision than human vision. Although this optical effect may have its origins in pollinator attraction, striations also occur in many cultivated varieties of tulip (table S1), which may have resulted from additional human selection for the luster that iridescence lends the flower.

Animals use iridescence for species recognition and mate selection (*1–4*), and iridescence is under selective pressure in some species—for example, arising from intraspecific competition between male butterflies in their attractiveness to females (*4*). Floral iridescence, in contrast, is presumably a signal to pollinating animals. Previous discussions about flower fluorescence show that a floral optical phenomenon, however intricate, must be demonstrated to have a biological signaling function (*19–21*). To test whether iridescence, as displayed by *H. trionum*, is distinguished by pollinators, we measured the variation in hue shown by the iridescent patch with spectroscopy both across the striations (measuring maximum iridescence) and along the striations (measuring minimum iridescence). The color loci of these two measurements were calculated in a bee hexagon color space [a representation of color perception designed using information about receptor sensitivity and color-opponent coding, so that distances between points generated by two objects indicate the degree to which the two are distinguishable (*22*)] (Fig. 4A). This indicated that bees will perceive a change in flower color from different angles. We observed that the difference in color between the two measurements, when calculated as the Euclidean distance between color loci, was 0.217. As a color distance of 0.15 is distinguishable by bees with above 90% accuracy, and even a distance of 0.05 can be distinguishable by trained bees (*23*), the variation in hue demonstrated by a single *H. trionum* flower viewed from different angles is sufficient for ready visual discrimination by bees.

We tested the ability of flower-naïve bumblebees to discriminate between iridescent and noniridescent disks (cast, respectively, on the plastic diffraction grating removed from the outer edge of a disassembled CD and on smooth molded plastic) by using differential conditioning (*24*). Colored disks were generated by adding 50 μg of

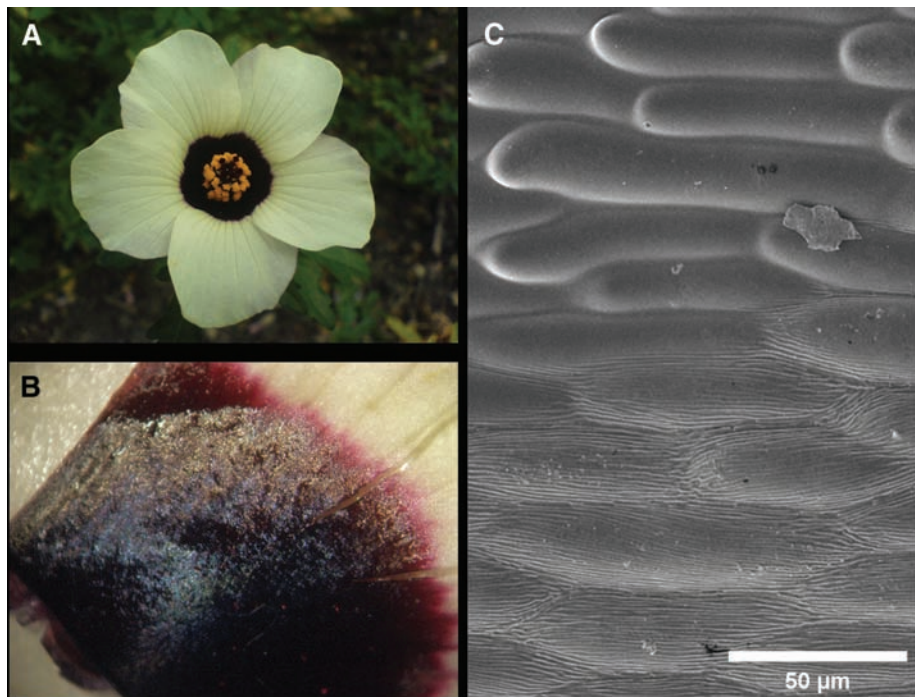Fig. 1. (**A**) *H. trionum* flower. (**B**) Base of *H. trionum* petal, showing iridescence overlying red pigment. (**C**) SEM of *H. trionum* petal, the upper half of the picture spanning the white (smooth cells) and the lower half spanning the pigmented (heavily striated longitudinally toward the petal base) epidermis.

Fig. 2. SEM images of tulip epoxy casts. (**A**) Top view showing striations on the petal surface of *T. kolpakowskiana*, resembling a line grating with a periodicity of 1.2 ± 0.3 μm. (**B**) Top view of an epoxy cast of a disassembled CD, showing a grating periodicity of 1.45 ± 0.05 μm. (**C**) Side view of the structure from (A), showing the rounded cross-section of the striation. The lower magnification image in (**D**) shows undulations with a periodicity of 29 ± 2 μm, reflecting the epidermal cells themselves. The insets in (A) and (B) show the optical appearance of the two gratings in transmission.
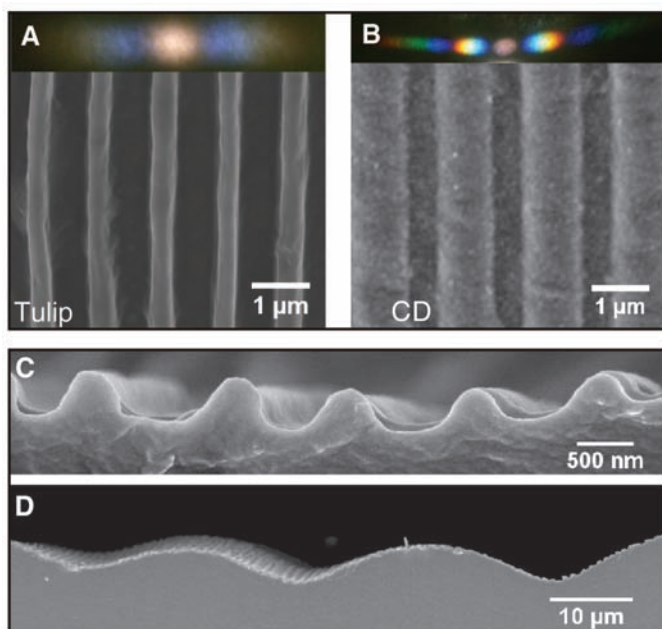
pigment (ultramarine blue, chrome yellow, manganese violet, or quinacridone red) to every 10 g of epoxy resin (fig. S4A).

We trained bees that iridescent disks containing yellow, blue, or violet pigment offered a sucrose reward, whereas identically pigmented noniridescent disks offered a bitter quinine hemisulphate salt solution (24). After 80 visits, bees visited iridescent disks more frequently than after their immediate introduction to the arena [first 10 visits = 4.7 ± 0.5 (mean ± SE); last 10 visits = 8.1 ± 0.4; Student's t test, t(9) =

4.96, P < 0.001] (Fig. 4B). Preference for iridescence did not differ according to pigment color (analysis of variance, $F_{2,16}$ = 1.57, P = 0.238). For each bee, these disks were then removed and replaced with five noniridescent and five iridescent red disks. When shown this previously unseen color, bees continued to visit iridescent flowers with 83.4 ± 3.4% accuracy [n = 10 bees; as compared with random choosing, t(9) = 5.72, P < 0.001] during their first foraging bout, demonstrating their ability to use iridescence as a cue to distinguish between rewarding and non-

rewarding substrates irrespective of pigment-based reflectance. This suggests that although pollinators are typically thought to identify rewarding flowers by their pigment-based reflectance, in our studies they were able to discriminate between the disks having a weak superposed angular-dependent color signal arising from grating interference.

The polarization of light reflected by iridescent colors on female *Heliconius* butterflies is recognized by males, but the changing colors are not (2). To assess if the visual cue used by the bumblebees was independent of a polarization effect, we repeated the discrimination experiment with only violet pigment disks and depolarizing Mylar over each disk. This removed polarization signals but left the color intact (2). Bees were again more likely to visit iridescent flowers as time progressed [mean visits ± SE; visits 1 to 10 = 4.3 ± 0.50; visits 71 to 80 = 9.2 ± 0.34; t(9) = 8.97, P < 0.001]. We repeated the experiment again with a polycarbonate filter opaque to wavelengths below 400 nm (25) blocking any UV signal, to ensure that the UV component of the diffraction grating was not acting as a specific cue. After 80 visits, bees visited iridescent disks more frequently than after their immediate introduction to the arena [first 10 visits = 4.9 ± 0.41; last 10 visits = 8.2 ± 0.25; t(9) = 8.10, P < 0.001] (learning curves shown in fig. S4B). We conclude that iridescence generated by diffraction gratings can be used as a pollination cue by bumblebees independent of underlying pigment, UV signals, or polarization effects.

To confirm that bees could discriminate the less regular iridescence of a real flower, yellow-pigmented epoxy casts were made from *T. kolpakowskiana* petals. Casts with floral iridescence were taken from the adaxial petal surface, which has striations, and casts without iridescence were taken from the abaxial petal surface, which lacks striations. Overall epidermal cell size and shape was similar on both surfaces. Our results show that bees were able to use the floral iridescence as accurately and effectively as they used the CD iridescence as a pollination cue. After 80 visits, bees visited iridescent disks more frequently than after their immediate introduction to the arena [first 10 visits = 4.8 ± 3.89 (mean ± SE), last 10 visits = 8.1 ± 3.14; t(9) = 5.75, P < 0.001] (Fig. 4B).

Over 50% of angiosperm species produce a striated cuticle over their petals (26), and although the degree to which such striations are ordered will strongly influence their visual effect, it is nonetheless probable that many flowers produce iridescence. We have so far identified 10 angiosperm families containing species with petal iridescence generated by diffraction gratings (table S2). Such striations may also influence pollinators through their tactile effects (27). As demonstrated by *H. trionum*, structures causing iridescence may occur in an overlying pattern to those caused by pigment color. This floral patterning is known to be important in pollinator attraction (18, 28). It has
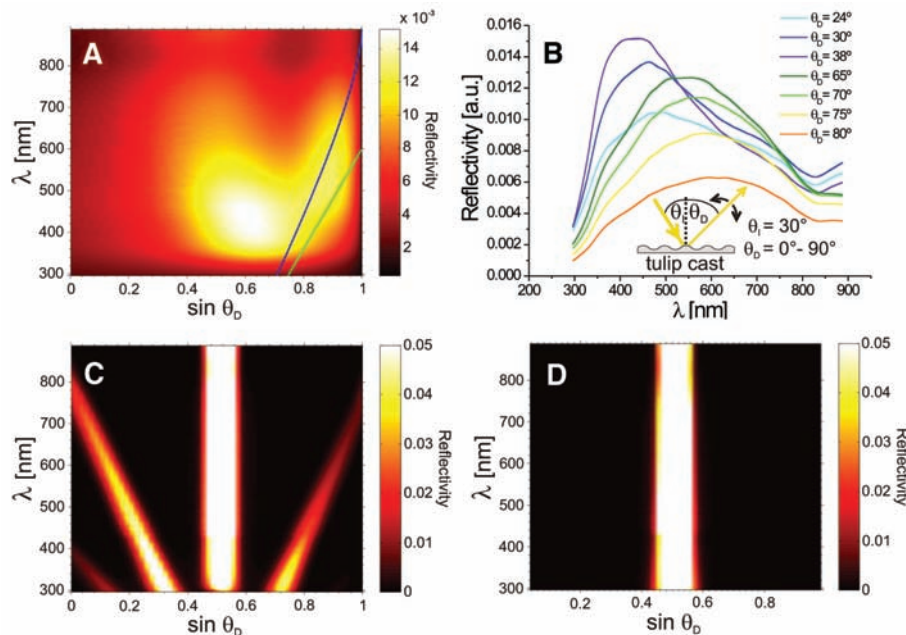

Fig. 3. Spectrally resolved reflection of the structures in Fig. 2. (**A**) Reflected intensity of the tulip cast [different representation in (**B**); a.u., arbitrary units] from Fig. 2A for θ_I = 30° as a function of sin θ_D and λ in comparison with (**C**) a CD cast (Fig. 2B) and (**D**) an unstructured surface. The central stripe in (**C**) and (**D**) is the signature of specular reflection. The two diagonal stripes in (**C**) are the first-order interference of the CD grating, with a weak second-order signal at the bottom left. The tulip cast in (**A**) shows the clear optical signature of an interference grating with a broadened first-order diffraction for sin θ_D > 0.7. The two lines are the delimiting predictions of the grating equation for a ~30-μm surface undulation leading to an inclination of the surface normal by −18° (blue) and 0° (green).
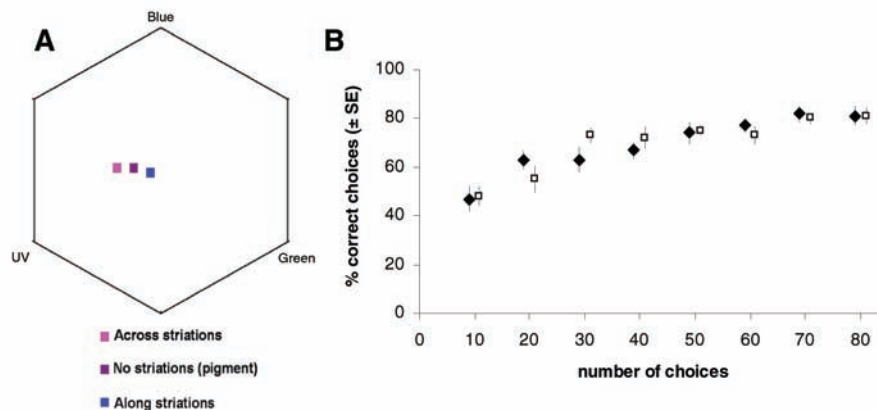

Fig. 4. Bee recognition of iridescent epoxy surfaces. (**A**) Loci of *H. trionum* in the bee color hexagon. (**B**) Two learning curves, each of 10 bees (with SE), choosing between rewarding iridescent flowers and nonrewarding noniridescent flowers. Filled diamonds indicate bees that were offered casts of CDs; clear squares indicate bees that were offered casts of tulip petals.

previously been shown in both birds and butterflies that structural color can enhance pigment color either by an additive or a contrast effect (8, 16, 29, 30). This interplay of structure and pigment may therefore also add to the diversity of pollination cues utilized by the flowers of many angiosperm species.

References and Notes

1. A. R. Parker, *J. Opt. A Pure Appl. Opt.* **2**, R15 (2000).
2. A. Sweeney, C. Jiggins, S. Johnsen, *Nature* **423**, 31 (2003).
3. R. L. Rutowski *et al.*, *Biol. J. Linn. Soc. London* **90**, 349 (2007).
4. D. J. Kemp, *Proc. R. Soc. London B Biol. Sci.* **274**, 1043 (2007).
5. N. I. Morehouse, P. Vukusic, R. L. Rutowski, *Proc. R. Soc. London B Biol. Sci.* **274**, 359 (2007).
6. A. R. Parker, Z. Hegedus, *J. Opt. A Pure Appl. Opt.* **5**, S111 (2003).
7. J. E. Kettler, *Am. J. Phys.* **59**, 367 (1991).
8. P. Kevan, W. Backhaus, in *Color Vision: Perspectives from Different Disciplines*, W. Backhaus, R. Kliegl, J. S. Werner, Eds. (Walter de Gruyter, Berlin, 1998), pp. 163–168.
9. K. Noda, B. Glover, P. Linstead, C. Martin, *Nature* **369**, 661 (1994).
10. H. Gorton, T. Vogelmann, *Plant Physiol.* **112**, 879 (1996).
11. C. Hebant, D. W. Lee, *Am. J. Bot.* **71**, 216 (1984).
12. T. C. Vogelmann, *Annu. Rev. Plant Physiol. Plant Mol. Biol.* **44**, 231 (1993).
13. P. B. Green, P. Linstead, *Protoplasma* **158**, 33 (1990).
14. C. Palmer, *Diffraction Grating Handbook* (Newport Corporation, Rochester, NY, ed. 6, 2005).
15. P. Skorupski, T. Döring, L. Chittka, *J. Comp. Physiol. A* **193**, 485 (2007).
16. R. L. Rutowski *et al.*, *Proc. R. Soc. London B Biol. Sci.* **272**, 2329 (2005).
17. P. Kevan, L. Chittka, A. Dyer, *J. Exp. Biol.* **204**, 2571 (2001).
18. K. Daumer, *Z. Vgl. Physiol.* **41**, 49 (1958).
19. F. Gandia-Herrero, F. Garcia-Carmona, J. Escribano, *Nature* **437**, 334 (2005).
20. R. Thorp, D. Briggs, J. Estes, E. Erickson, *Science* **189**, 476 (1976).
21. P. Kevan, *Science* **194**, 341 (1976).
22. L. Chittka, *J. Comp. Physiol. A* **170**, 533 (1992).
23. A. G. Dyer, L. Chittka, *Naturwissenschaften* **91**, 224 (2004).
24. H. M. Whitney, A. G. Dyer, L. Chittka, S. A. Rands, B. J. Glover, *Naturwissenschaften* **95**, 845 (2008).
25. P. L. Jokiel, R. H. York, *Limnol. Oceanogr.* **29**, 192 (1984).
26. Q. O. N. Kay, H. S. Daoud, C. H. Stirton, *Bot. J. Linn. Soc.* **83**, 57 (1981).
27. P. Kevan, M. Lane, *Proc. Natl. Acad. Sci. U.S.A.* **82**, 4750 (1985).
28. B. Heuschen, A. Gumbert, K. Lunau, *Plant Syst. Evol.* **252**, 121 (2005).
29. M. D. Shawkey, G. E. Hill, *Biol. Lett.* **1**, 121 (2005).
30. R. O. Prum, in *Bird Coloration, Mechanisms and Measurements*, G. E. Hill, K. J. McGraw, Eds. (Harvard Univ. Press, Boston, 2006), vol. 1, pp. 295–353.
31. We thank S. Rands, P. Rudall, R. Bateman, P. Cicuta, and J. Baumberg for discussions and Syngenta for bees. Funded by Natural Environment Research Council grant NE/C000552/1, Engineering and Physical Sciences Research Council grant EP/D040884/1, the European RTN-6 Network Patterns, the Cambridge University Research Exchange, and German Academic Exchange Service DAAD.

Real-Time DNA Sequencing from Single Polymerase Molecules

John Eid,* Adrian Fehr,* Jeremy Gray,* Khai Luong,* John Lyle,* Geoff Otto,* Paul Peluso,* David Rank,* Primo Baybayan, Brad Bettman, Arkadiusz Bibillo, Keith Bjornson, Bidhan Chaudhuri, Frederick Christians, Ronald Cicero, Sonya Clark, Ravindra Dalal, Alex deWinter, John Dixon, Mathieu Foquet, Alfred Gaertner, Paul Hardenbol, Cheryl Heiner, Kevin Hester, David Holden, Gregory Kearns, Xiangxu Kong, Ronald Kuse, Yves Lacroix, Steven Lin, Paul Lundquist, Congcong Ma, Patrick Marks, Mark Maxham, Devon Murphy, Insil Park, Thang Pham, Michael Phillips, Joy Roy, Robert Sebra, Gene Shen, Jon Sorenson, Austin Tomaney, Kevin Travers, Mark Trulson, John Vieceli, Jeffrey Wegener, Dawn Wu, Alicia Yang, Denis Zaccarin, Peter Zhao, Frank Zhong, Jonas Korlach,† Stephen Turner†

We present single-molecule, real-time sequencing data obtained from a DNA polymerase performing uninterrupted template-directed synthesis using four distinguishable fluorescently labeled deoxyribonucleoside triphosphates (dNTPs). We detected the temporal order of their enzymatic incorporation into a growing DNA strand with zero-mode waveguide nanostructure arrays, which provide optical observation volume confinement and enable parallel, simultaneous detection of thousands of single-molecule sequencing reactions. Conjugation of fluorophores to the terminal phosphate moiety of the dNTPs allows continuous observation of DNA synthesis over thousands of bases without steric hindrance. The data report directly on polymerase dynamics, revealing distinct polymerization states and pause sites corresponding to DNA secondary structure. Sequence data were aligned with the known reference sequence to assay biophysical parameters of polymerization for each template position. Consensus sequences were generated from the single-molecule reads at 15-fold coverage, showing a median accuracy of 99.3%, with no systematic error beyond fluorophore-dependent error rates.

The Sanger method for DNA sequencing (1) uses DNA polymerase to incorporate the 3'-dideoxynucleotide that terminates the synthesis of a DNA copy. This method relies on the low error rate of DNA polymerases, but exploits neither their potential for high catalytic rates nor high processivity (2–4). Increasing the speed and length of individual sequencing reads beyond the current Sanger technology limit will shorten cycle times, accelerate sequence assembly, reduce cost, enable accurate sequencing analysis of repeat-rich areas of the genome, and reveal large-scale genomic complexity (5, 6). Alternative approaches that increase sequencing performance have been reported [(7–10), reviewed in (11, 12)]. Several of these methods have been deployed as commercial sequencing systems (13–16), which have greatly increased overall throughput, enabling many applications that were previously unfeasible. However, because these methods all gate enzymatic activity, using various termination approaches, they have not yielded longer sequence reads (limited to ~400 nucleotides), nor do they exploit the high intrinsic rates of polymerase-catalyzed DNA synthesis.

The use of DNA polymerase as a real-time sequencing engine—that is, direct observation of processive DNA polymerization with base-pair resolution—has long been proposed but has been difficult to realize (7, 8, 17–22). To fully harness the intrinsic speed, fidelity, and processivity of these enzymes, several technical challenges must be met simultaneously. First, the speed at which each polymerase synthesizes DNA exhibits stochastic fluctuation, so polymerase molecules would need to be observed individually while they undergo template-directed synthesis. Because of the high nucleotide concentrations required by DNA polymerases (20), a reduction in the observation volume beyond what is afforded by conventional methods, such as confocal or total internal reflection microscopy, directly improves single-molecule detection. Second, deoxyribonucleoside triphosphate (dNTP) substrates must carry detection labels that do not inhibit DNA polymerization even when 100% of the native nucleotides are replaced with their labeled counterparts. Third, a surface chemistry is required that retains activity of DNA polymerase molecules and inhibits nonspecific adsorption of labeled dNTPs. Finally, an instrument is required that can faithfully detect and distinguish incorporation of four different labeled dNTPs. Here, we provide proof-of-concept for an approach to highly

Pacific Biosciences, 1505 Adams Drive, Menlo Park, CA 94025, USA.

*These authors contributed equally to this work.
†To whom correspondence should be addressed. E-mail: jkorlach@pacificbiosciences.com (J.K.); sturner@pacificbiosciences.com (S.T.)